Copper-64-diacetyl-bis(N^4-methylthiosemicarbazone): An agent for radiotherapy

Jason S. Lewis*, Richard Laforest*, Thomas L. Buettner†, Sheng-Kwei Song‡, Yasuhisa Fujibayashi§, Judith M. Connett†, and Michael J. Welch*¶

*Mallinckrodt Institute of Radiology and †Department of Surgery, Washington University School of Medicine, 510 South Kingshighway Boulevard, St. Louis, MO 63110; ‡Department of Chemistry, Washington University, St. Louis, MO 63110; and §Biomedical Imaging Research Center, Fukui Medical University, Matsuoka, Fukui 910-1193, Japan

Edited by Marcus E. Raichle, Washington University School of Medicine, St. Louis, MO, and approved December 7, 2000 (received for review August 21, 2000)

Systemic administration of hypoxia-selective ^{64}Cu-diacetyl-bis(N^4-methylthiosemicarbazone) (^{64}Cu-ATSM) has increased significantly the survival time of hamsters bearing human GW39 colon cancer tumors. Radiotherapy experiments were performed in animals bearing either 7-day-old (0.5–1.0 g) or 15-day-old (1.5–2.0 g) tumors. Studies compared animals treated with a single dose of 0, 4, 6, 7, 8, or 10 mCi of ^{64}Cu-ATSM (1 Ci = 37 GBq) with or without the vasodilator hydralazine. A multiple dose regimen of 3 × 4 mCi at 72-h intervals was studied also. Single doses of >6 mCi of ^{64}Cu-ATSM and the dose-fractionation protocol significantly increased the survival time of the hamsters compared with controls. The highest dose, 10 mCi of ^{64}Cu-ATSM, increased survival to 135 days in 50% of animals bearing 7-day-old tumors, 6-fold longer than control animals' survival (20 days), with only transient leucopenia and thrombocytopenia but no overt toxicity. Human absorbed doses were calculated from hamster biodistribution; the dose-critical organs were the lower large intestine (1.43 ± 0.19 rad/mCi) and upper large intestine (1.20 ± 0.38 rad/mCi). High-resolution MRI and positron-emission tomography using a therapeutic administration of 10 mCi were used to monitor tumor volume and morphology and to assess tumor dosimetry accurately, giving a tumor dose of 81 ± 7.5 rad/mCi. ^{64}Cu-ATSM has increased the survival time of tumor-bearing animals significantly with no acute toxicity and thus is a promising agent for radiotherapy.

Radiotherapy of cancer cells using cytotoxic radionuclides has wide application in basic research and clinical practice (1, 2). Antibody- and peptide-based radiotherapy agents have the advantages of specifically and selectively targeting cancer cells through overexpressed or unique antigens or receptors. Most success with antigen-based agents has been in treating hematological malignancies (3, ‖). However, these agents have only limited clinical success in treating solid tumors because of heterogeneous antigen expression among tumor cells and low overall tumor uptake.

Tumor resistance to therapy can be correlated , in part, to the development of hypoxic regions (areas of low oxygen tension; ref. 4). Hypoxic areas have been shown to be resistant to traditional chemotherapy because of hypoxia's effects on induced genes and by reducing the ability of the drug to create oxygen free radicals (5–7), which also protects from lethal effects of conventional ionizing radiation therapy (5, 6). However, high linear electron-transfer radiation such as α particles can kill cells effectively independent of cellular oxygenation. Creating hypoxia-selective small molecules, labeled with useful emissions, would provide a noninvasive method to treat resistant tumors. It is proposed that delivery of ^{64}Cu to a hypoxic cell could have such an effect because of its decay properties.

A number of metal-based small molecules have been suggested as agents for cancer radiotherapy. For example, metal-oxime chelates with ^{99m}Tc, ^{186}Re, ^{188}Re, ^{67}Cu, and ^{107}Ag (8) and rhenium-labeled hormones (9) have been suggested, but no preclinical or clinical data have been reported. This current work details an approach using dithiosemicarbazone complexes of radioactive Cu. The antitumor properties of dithiosemicarbazones were discovered in the 1960s (10), and the antitumor activity of the Cu(II) complexes of these ligands was greater than the ligands alone (11). With Cu radioisotopes, these neutral lipophilic Cu(II)bis(thiosemicarbazones) demonstrated rapid diffusion into cells and trapping of Cu ions (12, 13). Evaluation *in vitro* and *in vivo* showed uptake that is either nonhypoxia-selective (e.g., Cu-pyruvaldehyde-bis(N^4-methylthiosemicarbazone) or hypoxia-selective [e.g., ^{64}Cu-diacetyl-bis(N^4-methylthiosemicarbazone) (Cu-ATSM)] (14–16). These agents, labeled with copper radionuclides, have been evaluated as radiopharmaceuticals for myocardial and cerebral perfusion imaging, delineating hypoxia with positron-emission tomography (PET) and examining mitochondrial dysfunction (12, 14, 15, 17). The hypoxia selectivity of Cu-ATSM (Fig. 1) has been proven *in vivo* in animal tumor models (14), and preliminary clinical studies with ^{60}Cu-ATSM show it to be a noninvasive selective diagnostic marker for hypoxia in human cancers.**,††,‡‡

Copper-64 [$t_{1/2}$ = 12.7 h; E_{β^+max} = 0.653 million electronvolts (MeV) (17.4%); E_{β^-max} = 0.574 MeV (40%)] is a readily available cyclotron-produced positron-emitting isotope (18) with utility in diagnostic medicine (19) and promise as a therapeutic radionuclide because of its favorable β^- particle emissions (20, 21). It possesses similar lethality to ^{67}Cu whether free or complexed (22, 23). Agents based on Cu(II)-bis(thiosemicarbazone) complexes, which are taken up into tumor cells rapidly and efficiently, would have potential as radiotherapeutic agents in cancer. Additionally, ^{64}Cu labeling allows accurate assessment of tumor dosimetry and treatment response by using PET.

^{64}Cu-ATSM is taken up into hypoxic cells preferentially over normoxic cells in tumors (14). As a consequence, there may be greater cell killing of the hypoxic cells within a tumor. The levels of hypoxia in tumors can be manipulated by using hydralazine, a vasodilator that increases blood flow to most organs but decreases blood flow to tumors, transiently and dramatically decreasing tumor oxygenation (24, 25). Because hydralazine increases tumor hypoxia, it also may improve retention of

---

This paper was submitted directly (Track II) to the PNAS office.

Abbreviations: ^{64}Cu-ATSM, ^{64}Cu-diacetyl-bis(N^4-methylthiosemicarbazone); PET, positron-emission tomography; MeV, million electronvolts (1 eV = 1.602×10^{-19} J).

¶To whom reprint requests should be addressed at: Mallinckrodt Institute of Radiology, Washington University School of Medicine, Campus Box 8225, 510 South Kingshighway Boulevard, St. Louis, MO 63110. E-mail: welchm@mir.wustl.edu.

‖DeNardo, S. J., DeNardo, G. L. & Meares, C. J. (1991) *J. Nucl. Med.* **32,** 984 (abstr.).

Chao, C., Bosch, W. R., Mutic, S., Cutler, P. D., Lewis, J. S., Mintun, M. A., Dehdashti, F. & Welch, M. J. (2000) *J. Nucl. Med.* **41, 284 (abstr.).

††Dehdashti, F., Mintun, M. A., Lewis, J. S., Govindan, R. & Welch, M. J. (2000) *J. Nucl. Med.* 41, 34 (abstr.).

‡‡Mintun, M. A., Berger, K. L., Dehdashti, F., Lewis, J. S., Chao, C. & Welch, M. J. (2000) *J. Nucl. Med.* **41,** 58 (abstr.).

The publication costs of this article were defrayed in part by page charge payment. This article must therefore be hereby marked "*advertisement*" in accordance with 18 U.S.C. §1734 solely to indicate this fact.

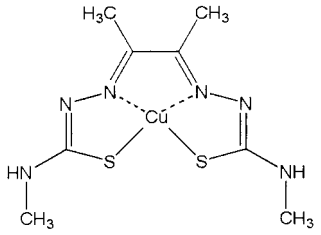

Fig. 1. Structure of Cu-ATSM.

Cu-ATSM, leading to a greater therapeutic response compared with nonhydralazine treated tumors. This present study addresses these hypotheses and evaluates the therapeutic efficacy of hypoxia-selective ^{64}Cu-ATSM in colorectal cancer by using a tumor-bearing hamster model with and without hydralazine.

Materials and Methods

^{64}Cu was produced on a CS-15 biomedical cyclotron at Washington University School of Medicine by using reported methods (18). ^{64}Cu-ATSM was synthesized by using previously described methods (16). All chemicals, unless otherwise stated, were purchased from Aldrich. All solutions were prepared by using distilled deionized water (Milli-Q, >18 MΩ resistivity; Millipore). Radiochemical purity of ^{64}Cu-ATSM in all studies was >98%.

Animal Models. Animal experiments were conducted in compliance with the Guidelines for the Care and Use of Research Animals established by Washington University's Animal Studies Committee. Male Golden Syrian hamsters (7 to 9 weeks old; Sasco Inc., Omaha, NE) were implanted with GW39 human colorectal carcinoma tumors in the thigh muscle as described (23). Animals were injected with vehicles or a tracer by cardiac puncture whilst under halothane anesthesia. Cardiac-puncture administration in hamsters has been adopted in our facilities and permits comparison to previous agents. In some animals, hydralazine was administered intraperitoneally 1 h before radioactivity at 5 mg/kg in a saline vehicle (1 mg/ml) to increase hypoxia transiently within the tumor before administration of radioactivity.

Therapy Studies. Radiotherapy experiments were performed in animals bearing either 7-day-old (0.5–1.0 g) or 15-day-old (1.5–2.0 g) tumors. Studies compared animals treated with a single administration of 0, 4, 6, 7, 8, or 10 mCi of ^{64}Cu-ATSM (1 Ci = 37 GBq) with or without hydralazine. The first study followed the survival of three groups of animals with 7-day-old tumors, which were those that received only hydralazine, only 10 mCi of ^{64}Cu-ATSM, or hydralazine plus 10 mCi of ^{64}Cu-ATSM. Another similar study tested a multiple-dose regimen of 3 × 4 mCi at 72-h intervals. A third study in animals with 7-day-old tumors compared the efficacy of 6, 8, or 10 mCi of ^{64}Cu-ATSM with no hydralazine. A similar dose-titration study with 15-day-old tumors was done to determine the radioactivity required to increase survival significantly. Throughout the experiment with 7-day-old tumors treated with 10 mCi of ^{64}Cu-ATSM, the tumor volume was monitored by direct calculation of the tumor volume by MRI. Each study was ended at 135 days after drug administration or a tumor burden of 10 g, whichever occurred earlier.

Statistical Analysis. To compare survival among different treatment groups, the SAS Lifetest procedure (26) was used to generate Kaplan–Meier probability density plots, and these data then were analyzed by using log-rank, Wilcoxon test, and −2log (LR) statistics and the P values are reported. Survival of each group at 135 days after injection was compared, and $P < 0.05$ was considered significantly different.

Toxicity. The Diagnostic Services Laboratory in the Department of Comparative Medicine at Washington University School of Medicine performed toxicity analyses. Physical appearance and hematologic, liver, and kidney chemistries for the tumor-bearing hamsters that received 10 mCi of ^{64}Cu-ATSM were compared with those from hamsters treated with control agents. The hematology analysis included total protein, hemoglobin, white blood cell counts (WBCs), red blood cell counts, platelet counts, hematocrit, and differential WBCs. Liver and kidney analysis included blood urea nitrogen, creatinine, alanine aminotransferase, and aspartate aminotransferase counts. The tumors were examined histologically at 135 days *ex vivo* by using hematoxylin-eosin and Mucin-staining techniques (27).

MRI and PET Imaging. Response to ^{64}Cu-ATSM treatment was monitored weekly by using T_2- and diffusion-weighted MRI. In four animals with 7-day-old tumors, 10 mCi of ^{64}Cu-ATSM was injected by cardiac puncture after the baseline T_2-weighted MRI. Then, 10-min static PET imaging was performed on a Siemens ECAT EXACT HR$^+$ Scanner 24 and 48 h after injection. This scanner has a large axial field of view (15.52-cm) with a spatial resolution of 4.5 mm full-width half-maximum at center. The field of view is sectioned into 63 transaxial planes. The MRI protocol was performed at days 1, 2, and 7 days and weekly afterward for 8 weeks on an Oxford Instruments 200/330 (4.7 tesla, 33-cm clear bore) magnet equipped with a 16-cm inner diameter actively shielded gradient coil (18 G/cm, 400-μsec rise time). The magnet, gradient coil, and power supply were interfaced with a Varian UNITY-INOVA console controlled by a Sun Microsystems Ultra-170 SPARC workstation (TE = 50 msec, TR = 3 sec, field of view = 4 × 4 cm, 1-mm slice, 256 × 256 pixels). The entire tumor mass was measured regardless of whether tissue was necrotic or healthy.

Dosimetry. Estimated human-absorbed doses of ^{64}Cu-ATSM to normal organs were calculated by using biodistribution data in nontumor-bearing hamsters according to described methods (21, 28). ^{64}Cu-ATSM (35 μCi, 1.3 MBq) was injected by cardiac puncture, and the hamsters were killed at 1, 3, 6, 12, 24, 36, or 48 h after injection. Animals for the 48-h time point were housed in metabolism cages to determine percentage of injected dose excreted in urine and feces at 1, 3, 6, 17, 24, 43, and 48 h. Time-activity curves (TACs) were generated for 12 organs. Cumulative activity (μCi/h or kBq/h) was determined by calculating the area under the TACs. Human-dose estimates then were calculated by using standard medical internal-radiation dose techniques, and S-values (mean absorbed dose per unit cumulative activity) for ^{64}Cu were obtained from the MIRDOSE3 program (29). Bone activity was assumed to be distributed equally between the trabecular bone and cortical bone.

Tumor Dosimetry. The absorbed dose to the GW39 tumor was determined from biodistribution data and by PET imaging. In the biodistribution method, tumor-uptake values from all time points after injection were combined by using integration methods to provide time-activity data. A nontherapeutic amount of ^{64}Cu-ATSM (5 μCi) was administered to hamsters bearing 7-day-old GW39 tumors. At selected time points over 48 h (n = 5), each tumor was excised and weighed, and an S value was interpolated by using a power function fitted through S values calculated with MIRDOSE3 for spherical nodules of standard sizes (28). S values and absorbed fractions were in agreement with a reported result (23). The tumor S values were calculated also by

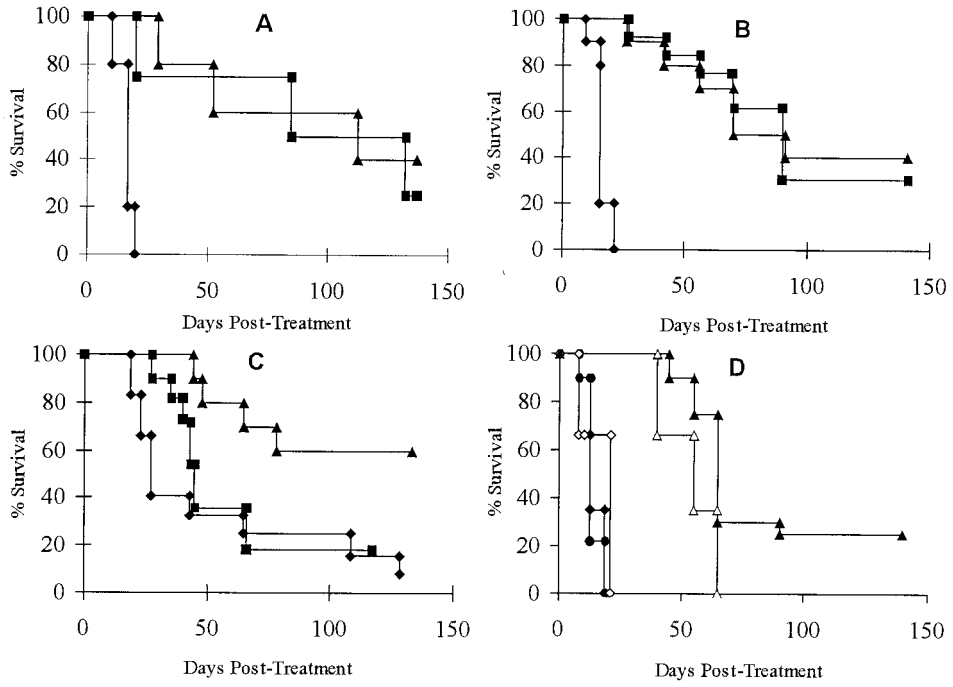

Fig. 2. Summary of therapy results obtained with the cardiac-puncture administration of ^{64}Cu-ATSM in hamsters bearing the GW39 carcinoma. Endpoint was 135 days or a tumor burden of 10 g, whichever came first. (*A*) Therapy of 7-day-old GW39 tumors in hamsters. Single administration of saline and hydralazine (♦, $n = 10$), 10 mCi of ^{64}Cu-ATSM without hydralazine (■, $n = 10$), or 10 mCi of ^{64}Cu-ATSM with hydralazine pretreatment (▲, $n = 9$). (*B*) Therapy of 7-day-old GW39 tumors in hamsters by using dose fractionation. Administration of saline, (♦, $n = 10$), 3×4 mCi of ^{64}Cu-ATSM at 72-h intervals without hydralazine (■, $n = 13$), or 3×4 mCi of ^{64}Cu-ATSM at 72-h intervals with hydralazine pretreatment (▲, $n = 13$). (*C*) Therapy of 7-day-old GW39 tumors in hamsters. Comparison of 10 (▲, $n = 10$), 8 (■, $n = 11$), and 6 (♦, $n = 12$) mCi. (*D*) Therapy of 15-day-old GW39 tumors in hamsters. Comparison of 4 (♦, $n = 7$), 6 (●, $n = 9$), 7 (◇, $n = 9$), 8 (△, $n = 9$), and 10 (▲, $n = 10$) mCi.

an electron-transport calculation (EGS4) and were in close agreement with those calculated by the MIRDOSE3 method above. Although alternative methods exist for calculating tumor dosimetry, it was preferable in this study to use MIRDOSE3 to simplify comparison with other previously reported ^{64}Cu-agents tested in the GW39 tumor model.

In the PET-plus-MRI study, hamsters bearing 7-day-old tumors ($n = 4$) were injected with a therapeutic amount of ^{64}Cu-ATSM (10 mCi) and were imaged by PET (10-min collection) and MRI (see above) at four time points over 48 h. Total uptake of ^{64}Cu-ATSM in the tumor was determined directly from the images by using reported methods and volume-of-interest techniques (28, 30). Tumor weight in each animal was determined by MRI assuming a tumor density of 1.04 g/cm^3. Then tumor S values were calculated with MIRDOSE3 nodule module as described above. Tumor dose was determined for each animal, and the weighted average was calculated.

Results

Therapy Studies. Therapy results are summarized in Fig. 2. Administration of 10 mCi of ^{64}Cu-ATSM to animals bearing 7-day-old tumors caused a 6-fold increase in survival (135 days) in 50% of the hamsters compared with controls (20 days, $P = 0.002$) (Fig. 2*A*). When compared with controls, a significant survival increase was seen also in the 10-mCi-of-^{64}Cu-ATSM and hydralazine group ($P = 0.0002$). However, survival time of ^{64}Cu-ATSM-treated animals was not affected by pretreatment with hydralazine ($P = 0.589$). ^{64}Cu-ATSM administered 3×4 mCi in 72-h intervals (Fig. 2*B*) also improved survival significantly compared with controls ($P = 0.0001$), but again hydralazine did not affect survival time ($P = 0.986$). In the first dose-titration study with 7-day-old tumors (Fig. 2*C*), there was no significant difference in survival for 6 or 8 mCi of ^{64}Cu-ATSM ($P = 0.665$), although both were significantly better than controls (6 mCi, $P = 0.014$; 8 mCi, $P = 0.005$). However, 10 mCi was superior compared with all groups (6 mCi, $P = 0.002$; 8 mCi, $P = 0.007$; controls, $P = 0.001$). In 15-day-old tumors (Fig. 2*D*), a dose of >6 mCi significantly increased survival time compared with controls ($P = 0.001$). All data sets were examined by using a regression analysis with the delivered dose as a continuous variable. The slope generated from this analysis was positive, indicating the trend that life expectancy increased with dose. Administration of H_2-ATSM or nonradioactive Cu-ATSM in amounts equivalent to those in the radioactive studies resulted in identical survival to the vehicle and hydralazine controls (data not shown).

Toxicity. Animals receiving 10 mCi of ^{64}Cu-ATSM displayed a transient depression in white blood cell count (WBC) and platelets. Toxicity was monitored further by weight loss and gross physical appearance, as well as hematologic, liver, and kidney function. The mean weight of the treated hamsters increased similarly to that of the control hamsters, and they maintained a healthy physical appearance (with no sign of scruffy coat or diarrhea) over the experimental period. Throughout the examination period, there were no significant changes in the total protein, hemoglobin, or red blood cell counts in any of the experimental or control groups. A 60% average decrease in WBC was noted after 3 days ($4{,}530 \pm 970/\text{mm}^3$ vs. $11{,}320 \pm 980/\text{mm}^3$) but recovered to baseline (control) levels by day 28 ($10{,}800 \pm 3{,}960/\text{mm}^3$). Platelet levels initially decreased to 25% of controls ($199 \pm 98 \times 10^3/\text{mm}$ vs. $778 \pm 149 \times 10^3/\text{mm}^3$) over the first 8 days after treatment but recovered to baseline by day 28 ($564 \pm 126 \times 10^3/\text{mm}^3$). The levels of kidney enzymes did not change significantly over the observation period. Levels of alanine aminotransferase and aspartate aminotransferase in-

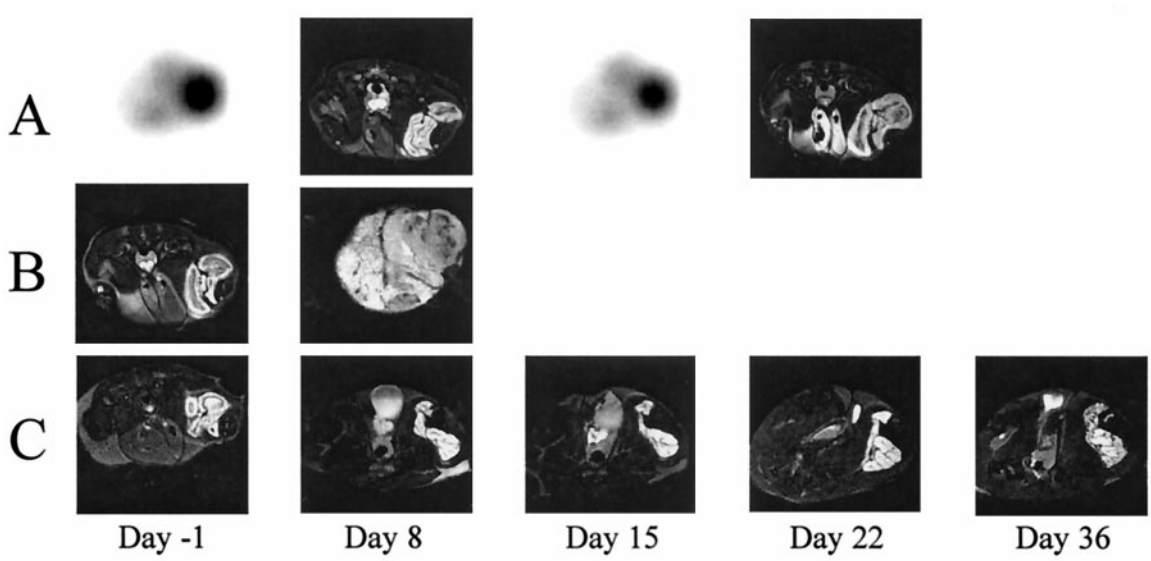

Fig. 3. (*A*) Transaxial PET images of ^{64}Cu-ATSM localized in the GW39 tumor 24-h after administration. Position of the tumor mass is confirmed by T_2-weighted MRIs of the same hamster in the same plane. (*B*) T_2-weighted transaxial MRI of two age-matched hamsters with the GW39 tumor in the thigh. The abnormal mass was still present 4 weeks after ^{64}Cu-ATSM treatment (*Left*). However, the age-matched tumor growth without the treatment (*Right*) resulted in a tumor nodule that occupied the entire thigh. (*C*) T_2-weighted MRI of a hamster with the GW39 tumor in the thigh. The abnormal mass was still present 5 weeks after ^{64}Cu-ATSM treatment but with little change in overall volume. The pitted appearance is noted in the tumor mass at 36 days, suggestive of a fibrotic response.

creased by 52 and 49% of controls, respectively, by day 3 after treatment but returned to baseline by day 8.

Histological examination (hematoxylin-eosin and Mucin staining) of tissue remaining at the site of tumor implantation exhibited extensive necrosis.

MRI and PET Imaging. The transaxial PET images show ^{64}Cu-ATSM localized in the GW39 tumor 24-h after administration (Fig. 3*A*). Position of the tumor mass was confirmed by T_2-weighted MRIs of the same hamster in the same plane. Abnormal tissue "tumor-like mass" was still present 8 weeks after treatment, but volume was not significantly different from day 1 after treatment. Animals receiving no treatment were killed by 4 weeks because of tumor burden (Fig. 3*B*). Increased signal intensity was observed in the T_2-weighted MRI beginning at day 1 after treatment. On day 36 after treatment, the T_2-weighted images showed changes in tumor heterogeneity: a "pitted" appearance suggestive of a fibrotic response appears (Fig. 3*C*). *Ex vivo* histological examination of this abnormal mass showed edema, lymphocyte infiltration, and extensive necrosis.

Dosimetry. The human-absorbed dose estimates to normal organs for ^{64}Cu-ATSM are shown in Table 1. The dose-critical organs are the lower large intestine (LLI) and upper large intestine (ULI). The values of 1.43 ± 0.19 rad/mCi (0.39 ± 0.05 mGy/MBq) for the LLI and 1.20 ± 0.38 rad/mCi (0.32 ± 0.10 mGy/MBq) for the ULI reflect the compound's primary clearance pathway through the liver. The liver received an absorbed dose of 0.69 ± 0.04 rad/mCi (0.19 ± 0.01 mGy/MBq).

Tumor Dosimetry. Tumor dose of ^{64}Cu-ATSM in hamsters with 7-day-old tumors was determined by two methods: biodistribution and PET imaging plus MRI. The maximum uptake of ^{64}Cu-ATSM into the GW39 tumor was 2.71 ± 0.26% injected dose per g at 4 h. When using data obtained from nontherapy biodistribution studies, the estimated therapeutic (10 mCi) dose delivered to the GW39 tumor was 57 ± 30 rad/mCi (15.4 ± 8.1 mGy/MBq). When extrapolating data obtained from PET and MRI of a therapeutic administration of 10 mCi of ^{64}Cu-ATSM, the tumor dose was similar at 81 ± 7.5 rad/mCi (21.9 ± 2.1 mGy/MBq; $P = 0.12$).

Discussion

^{64}Cu has been used for PET imaging (30, 31) and for radiotherapy (21, 23, 28). ^{64}Cu-labeled mAb 1A3 has similar lethality to ^{67}Cu-labeled mAb 1A3, and both Cu-labeled agents clearly exhibited complete tumor-growth inhibition in the established and widely used GW39 animal model of colorectal cancer (27). ^{64}Cu-labeled somatostatin-based peptides were taken up significantly in somatostatin-rich tissues in two tumor-bearing animal models and caused regression of CA20948 pancreatic tumors in rats (21, 28). Agents based on Cu(II)bis(thiosemicarbazone) complexes bypass the more common problems associated with using radiolabeled antibodies, with which success in treating solid tumors has been limited, because poor tumor uptake requires therapeutic doses that result in hematopoietic suppression (32, 33). The current investigation reports the therapeutic effectiveness of the hypoxia-selective agent ^{64}Cu-ATSM in a hamster tumor-bearing model.

Table 1. Human-absorbed radiation doses resulting from administration of ^{64}Cu-ATSM calculated from hamster biodistribution

Organ	^{64}Cu-ATSM	^{64}Cu-TETA-1A3
Kidneys	0.238 ± 0.008 (0.064)	0.329 (0.089)
Liver	0.693 ± 0.037 (0.187)	0.465 (0.126)
Bone surfaces	0.150 ± 0.003 (0.041)	0.216 (0.058)
Red marrow	0.101 ± 0.001 (0.027)	0.249 (0.067)
ULI wall	1.201 ± 0.383 (0.325)	0.508 (0.137)
Small intestine	0.405 ± 0.058 (0.109)	0.179 (0.048)
LLI wall	1.430 ± 0.186 (0.386)	0.475 (0.128)
Urinary bladder	0.072 ± 0.006 (0.019)	0.069 (0.019)
Total body	0.096 ± 0.001 (0.026)	

Comparison with ^{64}Cu-TETA-1A3 (23).

Absorbed doses are expressed as rad/mCi ± SD (mGy/MBq). ULI, upper large intestine; LLI, lower large intestine.

The results clearly demonstrate that ^{64}Cu-ATSM significantly increased survival of GW39 tumor-bearing hamsters compared with controls. This increase is impressive considering that GW39 tumors are not very responsive to a number of anticancer drugs and external X-irradiation (34), similar to human colorectal cancer. In addition, toxicity data indicate that the maximum tolerated dose (MTD) for this compound was not achieved, and larger quantities of radioactivity could be administered safely. Therefore, significant survival benefit was seen with less than the MTD of ^{64}Cu-ATSM. In all control groups, tumor burden reached the experimental endpoint of 10 g by 4 weeks. In contrast, in all animals receiving a dose greater than 6 mCi of ^{64}Cu-ATSM, tumor growth was inhibited and survival increased (Fig. 2). Animals with 7-day-old tumors receiving 10 mCi of ^{64}Cu-ATSM (± hydralazine) had a 50% survival rate at the 4-month experimental end point (merged data, Fig. 2 *A* and *C*).

Although it could be argued that larger tumors would have more hypoxic tissue and would therefore respond better than smaller tumors, survival at 4 months was just 30% when initial tumor burden was 1.5–2.0 g (15-day-old tumors; Fig. 2*D*). There are a number of possible explanations for this response. First, the larger tumor volume may reduce the effective concentration of ^{64}Cu-ATSM in hypoxic regions because of larger regions of necrosis leading to poor vascularization restricting the delivery of the agent to subtherapeutic levels. Further, ^{64}Cu emits a 0.58-MeV β^- particle (40%), a 0.66-MeV β^+ particle (19%), and a γ of 1.34 MeV (0.5%), giving a mean range of penetrating radiation of less than a millimeter in tissue; thus, ^{64}Cu emissions are more suitable for smaller tumor masses unless uniform distribution throughout the tissue is achieved.

In the multiple-dose protocol using ^{64}Cu-ATSM, overall survival was similar to the single-dose administration of 10 mCi and significantly longer than controls. Advantages of multiple-dose regimens over single-dose protocols have precedence in radioimmunotherapy (35, 36) and radiotherapy with peptides (28, 37). Fractionated doses deliver radiation over an extended period, which allows intermittent recovery of nontarget tissues, significantly reducing toxicity and increasing the tolerated tumor dose. However, the results presented here suggest the multiple-dose protocol and a 10 mCi single dose have similar effectiveness. Again, there are a number of possible explanations. First, the initial treatment in the multiple-dose regimen may kill significant amounts of the hypoxic regions. Because tumor volume remains static and new hypoxic region formation is unlikely, there could be relatively less hypoxia during subsequent doses, reducing their effectiveness. Furthermore, a different multidosing protocol may prove more effective than the single 10 mCi dose, which itself is not the maximum tolerated dose. To improve on the results reported here, optimization could be achieved by altering the dosing-time interval by using Cu-ATSM (labeled with the positron-emitting ^{60}Cu, ^{61}Cu, or ^{64}Cu) to delineate tumor hypoxia with PET and monitor changes in the hypoxic extent of tumors. After the first therapeutic dose, PET imaging will be performed regularly to determine when hypoxic levels are again significant. The next therapeutic dose of ^{64}Cu-ATSM then would be given, and so on.

Studies with a needle oxygen electrode have shown a decrease in tumor oxygenation after treatment with hydralazine (38). However, the current study showed that pretreatment with hydralazine did not increase survival significantly compared with nonhydralazine groups. It was expected that hydralazine-induced transient hypoxia would improve the therapeutic effectiveness of ^{64}Cu-ATSM. It is unclear why therapeutic effectiveness did not increase, but several confounding factors exist, including the vasodilatory effect in normal tissues reducing delivery of ^{64}Cu-ATSM to the tumor and the length of action of the drug. Additionally, altered pharmacokinetics of ^{64}Cu-ATSM following hydralazine treatment may contribute to these findings (38).

The human-absorbed dose estimates calculated from hamster biodistribution data show lower large intestine (LLI) and upper large intestine (ULI) to be the dose-critical organs, primarily because of hepatobiliary excretion. Comparison of the calculated doses for ^{64}Cu-ATSM and ^{64}Cu-TETA-1A3 is in Table 1. The calculated ^{64}Cu-ATSM absorbed doses to the hepatobiliary system are higher than those for ^{64}Cu-TETA-1A3, but other nontarget organs such as kidney and bone are lower than for the antibody. In the present therapeutic study, a single dose of 10 mCi ^{64}Cu-ATSM was administered to tumor-bearing hamsters, which weighed approximately 100 g, suggesting a dose of 7,500 mCi of ^{64}Cu-ATSM for clinical therapy trials in humans. This extrapolates to absorbed doses of 10,725 rad (107.25 Gy) to LLI wall, 9,007 rad (90.07 Gy) to ULI wall, and 5,197 rad (51.97 Gy) to liver. Fractionation might reduce the absorbed doses to nontarget organs significantly by allowing the delivery of a consistent amount of tolerable radiation over an extended period to the tumor, while allowing intermittent recovery of nontarget tissues. Laxatives can also be used to help reduce the absorbed doses to the intestines. It is also important to note that hepatobiliary and renal clearance of many radiopharmaceuticals vary widely from rodents to humans (39), and primate and human data may improve dose estimates.

The dose of ^{64}Cu-ATSM to 7-day-old tumors was calculated in two ways: by biodistribution studies and PET plus MRI. Biodistribution experiments performed with a nontherapeutic tracer level of radioactivity result in continued tumor growth throughout the study, whereas in therapy studies, tumor volumes are static or decrease. Because tracer biodistribution may differ from biodistribution of therapeutic quantities, using tracer biodistribution data could estimate tumor dose delivered in a therapy study inaccurately. From biodistribution data, we calculated a tumor dose of 57 ± 30 rad/mCi (15.4 ± 8.1 mGy/MBq). PET plus MRI with a therapeutic amount of radioactivity (10 mCi) gave a tumor dose of 81 ± 7.5 rad/mCi (21.9 ± 2.1 mGy/MBq). Although these values are not significantly different ($P = 0.12$), using PET plus MRI allowed us to calculate tumor dose from a therapeutic administration and monitor tumor volume over time, which may produce a more realistic tumor dose of ^{64}Cu-ATSM. Monitoring tumor volume during therapy allows tumor-absorbed doses to be calculated individually before averaging, a situation not possible in biodistribution.

The tumor dose of 81 ± 7.5 rad/mCi (21.9 ± 2.1 mGy/MBq) for ^{64}Cu-ATSM is lower than the dose of 110 rad/mCi (29.7 mGy/rad) calculated for radioimmunotherapy of smaller GW39 tumors with 3 mCi of ^{64}Cu-labeled 1A3 (23). Another study showed that 7 mCi of internalizing ^{64}Cu-labeled 1A3 (770 rad, 7.7 Gy) gave 40% survival (8 of 20) 4 months after treatment of 7-day-old tumors (40), comparable to the current study (merged data, Fig. 2 *A* and *C*) in which 10 mCi of ^{64}Cu-ATSM (810 rad, 8.1 Gy) gave 50% survival (10 of 20) at 4 months. Therefore, similar delivered doses of either ^{64}Cu-BAT-2IT-1A3 or ^{64}Cu-ATSM gave comparable responses in tumor-bearing hamsters. ^{67}Cu-BAT-2IT-1A3 (706 rads, 7.06 Gy) in 0.6-g GW39 tumors gave similar results to ^{64}Cu-ATSM. With ^{131}I-labeled mAb-NP4 in 0.3- to 0.45-g tumors, a 55% tumor remission was noted when 7,200 rad (72 Gy) was delivered (41).

Subcellular fractionation studies show that a significant portion of the analog ^{64}Cu-pyruvaldehyde-bis(N^4-methylthiosemicarbazone is delivered to the cell nucleus (>20% after 24 h; ref. 42, §§). It is reasonable that intracellular reduction of ^{64}Cu(II)-ATSM to ^{64}Cu(I)-ATSM might lead eventually to the translocation of copper to the nucleus in a similar manner. The binding of Cu(II) to DNA and/or other structures in the nucleus has been established firmly, and an important role for the Cu ion in maintaining nuclear matrix organization and DNA folding has been suggested (43). Chiu *et al.* found that treatment of isolated nuclei with low levels of Cu(II) causes nuclear matrix-associated-DNA binding to nuclear matrix proteins and DNA–protein crosslinking, as well as DNA double-strand breaks after irradi-

§§Shibuya, K., Fujibayashi, Y., Sasai, K., Hiraoka, K. & Konishi, J. (1997) *J. Nucl. Med.* **38,** 183 (abstr.).

ation (44). ^{64}Cu decays 40% by electron capture, emitting Auger electrons with high linear electron transfer. Radiotoxic Auger electrons have a tissue penetration of 0.02–10 μm with very high toxicity if the DNA of the cell is within range (45). ^{64}Cu emits a 6.84-keV Auger electron with a penetration range of about 5 μm, the approximate cell-nucleus diameter. Moreover, the maximum recoil energy from the transmutation of ^{64}Cu (from β^- = 7.6 eV; from β^+ = 9.15 eV) (46) to its highly charged daughter nucleus may also increase the cell-killing ability. The combination of these characteristics with the likely event ^{64}Cu is bound to certain structures within the nucleus increase its toxicity. Additionally, Auger- and recoil-linked toxicity would be as great in hypoxic cells as in oxygenated.

Because low-energy Auger electrons deposit their energy in a very small volume and the ^{64}Cu is likely very close to DNA, conventional macroscopic dose calculations are likely to underestimate the energy imparted and thus the dose. A microdosimetric approach to the tumor-dose calculations, accounting for all Auger electrons, would raise estimates and relate more closely to the observed growth inhibition. Because of their short-range and relatively larger linear electron transfer, low-energy Auger electrons potentially are more radiotoxic than the higher-energy positron or β^- particle.

The PET plus MRI yielded information and data not normally available in radiotherapy experiments in rodents. Historically, tumor volumes have been calculated from caliper measurements. However, they provide no physiologic information during radiotherapy experiments, and their accuracy is limited by tumors' irregular shapes. In this study, MRI confirmed and quantified tumor mass and also indicated severe necrosis and a long reabsorption time. Caliper methods alone would have given incomplete information. Our results indicate PET plus MRI can help to monitor therapeutic response, determine overall treatment effectiveness, and permit accurate dosimetry calculations.

Radiotherapeutic effectiveness depends on radioligand delivery to, and accumulation in, the cell. Therefore, high accessibility and up-regulation of antigens or receptors is required for effective treatment by using peptide- or antibody-based agents but not ^{64}Cu-ATSM or other nonreceptor-based agents. Therapeutic quantities of hypoxia-selective ^{64}Cu-ATSM inhibited GW39 tumor growth in hamsters and significantly increased survival with no acute toxicity. The addition of ^{64}Cu to the radiotherapy arsenal is useful and innovative because it enables accurate monitoring of drug distribution and biokinetics through concurrent PET imaging. ^{64}Cu-ATSM has shown exceptional promise as a radiotherapy agent and could be used before, during, or after surgery to ablate "resistant" tumor regions before traditional treatments.

We thank Dr. William Connett for the statistical analysis and Drs. Joseph J. H. Ackerman and Carolyn J. Anderson for discussions. Thanks to Dr. Deborah W. McCarthy and Todd A. Perkins for ^{64}Cu production and to Terry Sharp, John Engelbach, and Suzanne Hickerson for technical assistance. Thanks to Dr. Joanna Downer for editorial help. We acknowledge the U. S. Department of Energy (DE-FG02-87ER60212) and the National Institutes of Health (1 R24 CA86307, 5 R24 CA83060) for funding.

1. Goldenberg, D. M. (1991) in *Cancer Imaging and Therapy with Radiolabeled Antibodies* (Plenum, New York), pp. 107–117.
2. Zuckier, L. S. & Denardo, G. L. (1997) *Semin. Nucl. Med.* **27,** 10–29.
3. Press, O. W., Eary, J. F., Appelbaum, F. R., Martin, P. J., Nelp, W. B., Glenn, S., Fisher, D. R., Porter, B., Matthews, D. C., Gooley, T., et al. (1995) *Lancet* **346,** 336–340.
4. Brown, J. M. (1999) *Cancer Res.* **59,** 5863–5870.
5. Crabtree, H. G. & Cramer, W. (1933) *Proc. R. Soc. London Ser. B.* **113,** 238–250.
6. Gray, L. H., Conger, A. D., Ebert, M., Hornsey, S. & Scott, O. C. (1953) *Br. J. Radiol.* **26,** 638–648.
7. Teicher, B. A., Holden, S. A., Al-Achi, S. A. & Herman, T. S. (1990) *Cancer Res.* **50,** 3339–3344.
8. Archer, C. M., Canning, L. R., Gill, H. K. & Riley, A. L. M. (1992) World Patent WO9409849-A.
9. Top, S., Vessieres, A., Jaouen, G. & Quivy, J. (1992) European Patent EP565449-A.
10. Petering, H. G., Buskirk, H. H. & Underwood, G. E. (1964) *Cancer Res.* **24,** 367–372.
11. Petering, D. H. (1972) *Bioinorg. Chem.* **1,** 255–271.
12. Green, M. A. (1987) *Nucl. Med. Biol.* **14,** 59–61.
13. Fujibayashi, Y., Wada, K., Taniuchi, H., Yonekura, Y., Konishi, J. & Yokoyama, A. (1993) *Biol. Pharm. Bull.* **16,** 146–149.
14. Lewis, J. S., McCarthy, D. W., McCarthy, T. J., Fujibayashi, Y. & Welch, M. J. (1999) *J. Nucl. Med.* **40,** 177–183.
15. Taniuchi, H., Fujibayashi, Y., Yonekura, Y., Konishi, J. & Yokoyama, A. (1997) *J. Nucl. Med.* **38,** 1130–1134.
16. Fujibayashi, Y., Cutler, C. S., Anderson, C. J., McCarthy, D. W., Jones, L. A., Sharp, T., Yonekura, Y. & Welch, M. J. (1999) *Nucl. Med. Biol.* **26,** 117–121.
17. Dearling, J. L. J., Lewis, J. S., Welch, M. J., McCarthy, D. W. & Blower, P. J. (1998) *Chem. Commun.* **22,** 2531–2533.
18. McCarthy, D. W., Shefer, R. E., Klinkowstein, R. E., Bass, L. A., Margeneau, W. H., Cutler, C. S., Anderson, C. J. & Welch, M. J. (1997) *Nucl. Med. Biol.* **24,** 35–43.
19. Blower, P. J., Lewis, J. S. & Zweit, J. (1996) *Nucl. Med. Biol.* **23,** 957–980.
20. Anderson, C. J., Schwarz, S. W., Connett, J. M., Cutler, P. D., Guo, L. W., Germain, C. J., Philpott, G. W., Zinn, K. R., Greiner, D. P., Meares, C. F. & Welch, M. J. (1995) *J. Nucl. Med.* **36,** 850–858.
21. Lewis, J. S., Lewis, M. R., Cutler, P. D., Srinivasan, A., Schmidt, M. A., Schwarz, S. W., Morris, M. M., Miller, J. P. & Anderson, C. J. (1999) *Clin. Cancer. Res.* **5,** 3608–3616.
22. Apelgot, S., Coppey, J., Gaudemer, A., Grisvard, J., Guille, E., Sasaki, I. & Sissoeff, I. (1989) *Int. J. Radiat. Biol.* **55,** 365–384.
23. Connett, J. M., Anderson, C. J., Guo, L. W., Schwarz, S. W., Zinn, K. R., Rogers, B. E., Siegel, B. A., Philpott, G. W. & Welch, M. J. (1996) *Proc. Natl. Acad. Sci. USA* **93,** 6814–6818.
24. Voorhees, W. D. & Babbs, C. F. (1982) *Eur. J. Cancer Clin. Oncol.* **19,** 1027–1033.
25. Chaplin, D. J. (1989) *J. Natl. Cancer Inst.* **81,** 618–622.
26. SAS (1990) *SAS/STAT Users Guide* (SAS Institute, Cary, NC) 4th Ed., Vol 2.
27. Wu, J. S., Brasfield, E. B., Guo, L.-W., Ruiz, M., Connett, J. M., Philpott, G. W., Jones, D. B. & Fleshman, J. W. (1997) *Surgery (St. Louis)* **122,** 1–7.
28. Anderson, C. J., Jones, L. A., Bass, L. A., Sherman, E. L. C., McCarthy, D. W., Cutler, P. D., Lanahan, M. V., Cristel, M. E., Lewis, J. S. & Schwarz, S. W. (1998) *J. Nucl. Med.* **39,** 1944–1951.
29. Stabin, M. (1996) *J. Nucl. Med.* **37,** 538–546.
30. Cutler, P. D., Schwarz, S. W., Anderson, C. J., Connett, C. J., Welch, M. J., Philpott, G. W. & Siegel, B. A. (1995) *J. Nucl. Med.* **36,** 2363–2371.
31. Philpott, G. W., Schwarz, S. W., Anderson, C. J., Dehdashti, F., Connett, J. M., Zinn, K. R., Meares, C. F., Cutler, P. D., Welch, M. J. & Siegel, B. A. (1995) *J. Nucl. Med.* **36,** 1818–1824.
32. Buchsbaum, D. J., Langmuir, V. K. & Wessels, B. W. (1993) *Med. Phys.* **20,** 551–567.
33. DeNardo, G. L. & DeNardo, S. J. (1995) in *Cancer Therapy with Radiolabeled Antibodies* (CRC, London), pp. 217–227.
34. Goldenberg, D. M. & Ammersdorfer, E. (1970) *Eur. J. Cancer* **6,** 73–80.
35. DeNardo, G. L., Denardo, S. J., O'Grady, L. F., Levy, N. B., Adams, G. P. & Mills, S. L. (1990) *Cancer Res.* **50,** Suppl. 1014–1016.
36. Kwa, H. B., Verhoeven, A. H. M., Storm, J., Vanzandwijk, N., Mooi, W. J. & Hilkens, J. (1995) *Cancer Immunol. Immunother.* **41,** 169–174.
37. Zamora, P. O., Gulhke, S., Bender, H., Diekmann, D., Rhodes, B. A., Biersack, H.-J. & Knapp, F. F. (1996) *Int. J. Cancer* **65,** 214–220.
38. Lewis, J. S., Sharp, T. L., Jones, L. A., Fujibayashi, Y. & Welch, M. J. (2001) *J. Nucl. Med.*, in press.
39. Fritzberg, A. R. & Bloedow, D. C. (1983) in *Animal Models in Radiotracer Design*, eds. Lambrecht, R. M. & Eckelman, W. C. (Springer, New York) pp.179–209.
40. Connett, J. M., Buettner, T. L. & Anderson, C. J. (1999) *Clin. Cancer Res.* **5,** 3207–3212.
41. Blumenthal, R., Sharkey, R., Kashi, R. & Goldenberg, D. (1989) *Int. J. Cancer* **44,** 292–300.
42. Baerga, I. D., Maickel, R. P. & Green, M. A. (1992) *Nucl. Med. Biol.* **19,** 697–701.
43. George, A. M., Sabovljev, S. A., Hart, L. E., Cramp, W. A., Harris, G. & Hornsey, S. (1987) *Br. J. Cancer* **55,** Suppl. 8, 141–144.
44. Chiu, S.-M., Xue, L.-Y., Friedman, L. R. & Oleinick, N. L. (1993) *Biochemistry* **32,** 6214–6219.
45. Adelstein, S. J. (1993) *Am. J. Roentgenol.* **160,** 707–713.
46. Wahl, A. C. & Bonner, N. A., eds. (1958) *Radioactivity Applied to Chemistry*, (Wiley, London), pp. 511–514.